



## Development of Goss texture in Al–0.3%Cu annealed after heavy rolling

**Shuai, L. F.; Huang, T. L.; Wu, G. L.; Huang, X.; Mishin, O. V.**

*Published in:*  
Journal of Alloys and Compounds

*Link to article, DOI:*  
[10.1016/j.jallcom.2018.03.187](https://doi.org/10.1016/j.jallcom.2018.03.187)

*Publication date:*  
2018

*Document Version*  
Peer reviewed version

[Link back to DTU Orbit](#)

*Citation (APA):*  
Shuai, L. F., Huang, T. L., Wu, G. L., Huang, X., & Mishin, O. V. (2018). Development of Goss texture in Al–0.3%Cu annealed after heavy rolling. *Journal of Alloys and Compounds*, 749, 399-405.  
<https://doi.org/10.1016/j.jallcom.2018.03.187>

---

### General rights

Copyright and moral rights for the publications made accessible in the public portal are retained by the authors and/or other copyright owners and it is a condition of accessing publications that users recognise and abide by the legal requirements associated with these rights.

- Users may download and print one copy of any publication from the public portal for the purpose of private study or research.
- You may not further distribute the material or use it for any profit-making activity or commercial gain
- You may freely distribute the URL identifying the publication in the public portal

If you believe that this document breaches copyright please contact us providing details, and we will remove access to the work immediately and investigate your claim.

# Accepted Manuscript

Development of Goss texture in Al–0.3%Cu annealed after heavy rolling

L.F. Shuai, T.L. Huang, G.L. Wu, X. Huang, O.V. Mishin



PII: S0925-8388(18)31057-0

DOI: [10.1016/j.jallcom.2018.03.187](https://doi.org/10.1016/j.jallcom.2018.03.187)

Reference: JALCOM 45417

To appear in: *Journal of Alloys and Compounds*

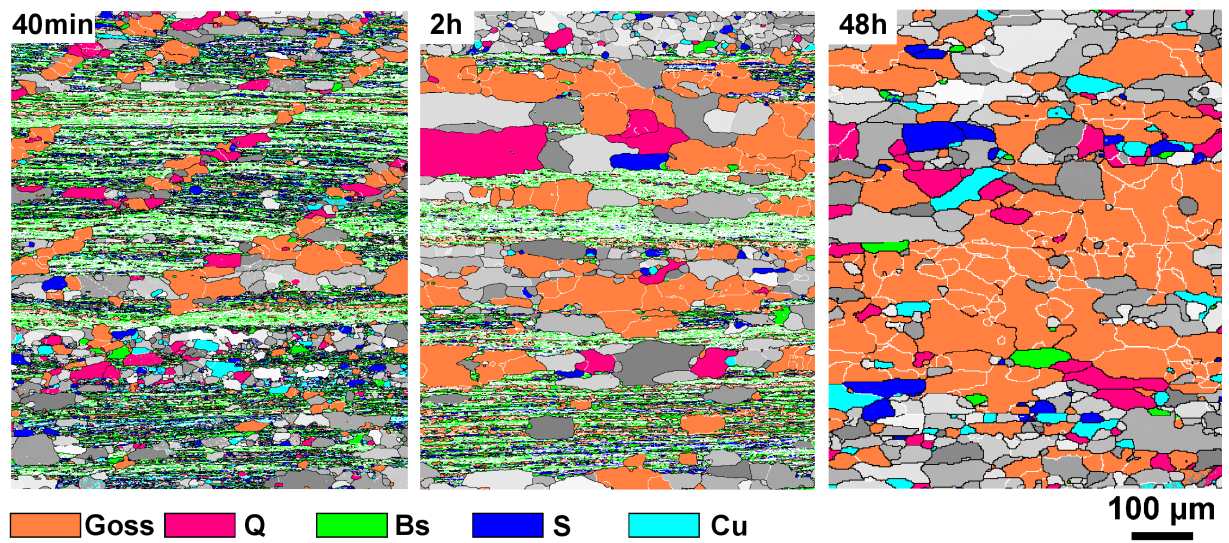
Received Date: 18 January 2018

Revised Date: 9 March 2018

Accepted Date: 14 March 2018

Please cite this article as: L.F. Shuai, T.L. Huang, G.L. Wu, X. Huang, O.V. Mishin, Development of Goss texture in Al–0.3%Cu annealed after heavy rolling, *Journal of Alloys and Compounds* (2018), doi: 10.1016/j.jallcom.2018.03.187.

This is a PDF file of an unedited manuscript that has been accepted for publication. As a service to our customers we are providing this early version of the manuscript. The manuscript will undergo copyediting, typesetting, and review of the resulting proof before it is published in its final form. Please note that during the production process errors may be discovered which could affect the content, and all legal disclaimers that apply to the journal pertain.

**Al-0.3%Cu annealed at 200 °C**

## Development of Goss texture in Al–0.3%Cu annealed after heavy rolling

L.F. Shuai<sup>1</sup>, T.L. Huang<sup>1,\*</sup>, G.L. Wu<sup>1,\*\*</sup>, X. Huang<sup>1,2</sup> and O.V. Mishin<sup>2</sup>

<sup>1</sup> College of Materials Science and Engineering, Chongqing University, Chongqing 400045, China

<sup>2</sup> Department of Mechanical Engineering, Technical University of Denmark, 2800 Kgs. Lyngby,

Denmark

### Abstract

The evolution of the microstructure and texture during annealing has been studied in the center layer of 95% cold rolled Al–0.3%Cu with a large initial grain size. The cold-rolled condition is characterized by a strong Brass texture component and a deformed microstructure comprising lamellar structures intersected by a large number of shear bands. Recrystallization and precipitation take place during annealing at 200 °C, and a strong Goss texture develops. In the beginning of recrystallization, Goss oriented grains nucleate preferentially at the shear bands. At a later stage of recrystallization, new Goss nuclei can appear in regions where lamellae of the dominant Brass component are interspersed with Goss-oriented subgrains. When recrystallization is almost complete, recrystallized Goss-oriented grains grow into grains of other orientations, which results in a rapid increase in the average grain size of Goss-oriented grains and strengthening of the Goss texture. As a result, new low angle boundaries are formed between Goss-oriented grains in this strongly textured material.

Keywords: aluminum alloys; cold rolling; annealing; recrystallization; Goss texture

---

\* Corresponding author. *E-mail address:* [huangtl@cqu.edu.cn](mailto:huangtl@cqu.edu.cn)

\*\*Corresponding author. *E-mail address:* [wugl@cqu.edu.cn](mailto:wugl@cqu.edu.cn)

## 1. Introduction

Depending on the chemical composition, homogenization and subsequent thermomechanical processing, different annealing textures can develop in rolled Al-alloys. The most commonly reported recrystallization texture component after heavy rolling in aluminum with a low concentration of impurities is the cube texture  $\{001\}\langle 100 \rangle$  [1–4]. However, in Al-alloys containing coarse particles the texture can be dominated by the P component, defined as either  $\{110\}\langle 111 \rangle$ ,  $\{110\}\langle 566 \rangle$  or  $\{110\}\langle 122 \rangle$  [4–9], which is typically attributed to particle stimulated nucleation. A so-called retained deformation texture can be produced during annealing when recrystallized grains have orientations of the rolling texture [1,4,10]. The Goss  $\{110\}\langle 001 \rangle$  texture along with a weaker Q  $\{013\}\langle 231 \rangle$  component has also been reported after annealing of heavily rolled Al-alloys [11–13]. Compared to the other “standard” rolling texture components, such as Copper (Cu)  $\{112\}\langle 111 \rangle$ , S  $\{123\}\langle 634 \rangle$  and Brass (Bs)  $\{110\}\langle 112 \rangle$ , the Goss orientation is a minor rolling texture component. Whenever this component is produced during recrystallization, it alters the rolling texture so much that the final texture can no longer be described as a retained deformation texture.

In previous studies of Al–1.8%Cu, it has been suggested that grains of the Goss and Q orientations nucleate at shear bands [4,11,12]. Furthermore, local orientation measurements in Al–1%Mg provided experimental evidence that grains of these orientations can indeed nucleate at shear bands [13]. However, quantitative microstructural analysis of such grains and their evolution during annealing has not been conducted in these early publications. It should also be noted that since nucleation at shear bands results in grains of different orientations, and since there can also be other types of nucleation sites, the Goss component in the recrystallization texture is combined with other

texture components. Therefore, reported volume fractions of the Goss component in the annealing texture are usually moderate [13,14].

A rather strong Goss component was found in our preliminary study [15] of a heavily rolled and subsequently annealed Al–0.3%Cu alloy. After recrystallization at 200 °C, the fraction of the Goss texture in this alloy was approximately 40%. The very limited microstructural analysis presented in [15] was insufficient to clearly understand how the deformed material evolved to produce such a strong Goss texture during annealing. Therefore, the purpose of the present work is to characterize in detail the development of this strong texture during isothermal annealing covering both nucleation and growth of Goss-oriented grains. Electron backscatter diffraction (EBSD) is used in this work to monitor the evolution of microstructure and texture starting from the as-rolled sample to a completely recrystallized material.

## 2. Experimental

The material used in this experiment was produced from 99.999% pure Al and oxygen-free high conductivity copper. The as-cast ingot contained 1.5 – 2 mm large grains and was forged at 200 °C to obtain a 50 mm thick plate suitable for cold rolling. X-ray texture measurements revealed different dominant orientations in specimens taken from several different regions of the forged material, thus reflecting the presence of very large grains of varying orientations. The only consistent result obtained from the different regions was an increased concentration of orientations near the Goss component [15]. The microstructural examination of the forged sample demonstrated that the initial grains could still be clearly identified in the microstructure and that they were subdivided by dislocation boundaries. The forged sample was cold-rolled by multiple passes to a final thickness of 2.5 mm, which corresponded to a reduction of 95% (von Mises strain  $\epsilon_{vM} = 3.4$ ). The rolled material was

inhomogeneous through the sample thickness, and could roughly be divided into 3 distinct layers, each with a thickness of approximately 1/3 of the sample thickness. All examinations in the present work were conducted for the center layer with a thickness of ~0.8 mm. The cold-rolled sample was annealed at 200 °C for different periods of time.

The microstructure was investigated using a Zeiss Supra 35 field emission gun scanning electron microscope equipped with a Channel 5 EBSD system and in a Zeiss AURIGA dual-beam SEM equipped with an AZtechKL EBSD package. The longitudinal section containing the rolling direction (RD) and the normal direction (ND) was prepared using mechanical polishing followed by electrolytic polishing. A step size of 25 nm or 30 nm was used for the EBSD analysis of the deformed microstructure, while larger step sizes were used for microstructural examinations of the annealed samples. Low angle boundaries (LABs) and high angle boundaries (HABs) in the EBSD data were defined as boundaries with misorientations  $\theta = 2\text{--}15^\circ$  and  $\theta \geq 15^\circ$ , respectively.

The energy stored in the deformed and recovered microstructure was calculated from the EBSD data as described by Godfrey et al. [16,17]. The specific boundary energy of the LABs was calculated from the Read–Shockley equation [18,19], whereas the specific boundary energy of HABs was assumed to be 0.324 J/m<sup>2</sup> [20]. Recrystallized grains were identified based on the method described in [21]. In the present work, such grains were defined as regions greater than 5  $\mu\text{m}$  with internal misorientations less than 1° surrounded by boundaries with  $\theta \geq 2^\circ$ . An additional criterion was that there should be at least one HAB segment among the boundaries between each recrystallized grain and its surrounding matrix.

Texture measurements of the rolled sample and each annealed sample were conducted using EBSD with a step size of 10  $\mu\text{m}$  and covering several millimeters along the RD and the entire thickness

of the center layer. Fractions of texture components were calculated applying a  $15^\circ$  deviation from the closest exact  $\{hkl\}\langle uvw \rangle$  orientation.

Electrical conductivity was measured using a portable eddy-current conductivity meter D60K. The measurements were conducted on the rolling plane after grinding specimens to the mid-thickness and cleaning them with ethanol. Three measurements were performed for each specimen.

### 3. Results

#### 3.1 As-rolled material

The deformed microstructure contains finely spaced lamellar boundaries aligned parallel with the rolling plane and shear bands at  $\sim 30^\circ$  to the rolling direction (see Fig.1a). Bright features seen in Fig.1a,b along some boundaries are particles identified as  $Al_2Cu$ . The average spacing measured between the lamellar boundaries is  $\sim 250$  nm. The fraction of HABs determined using EBSD in this material is comparatively low,  $\sim 30\%$ .

EBSD data provide clear evidence that the rolling texture is dominated by the Bs component (Fig.1c). The area fraction of this texture component is 51%, while area fractions of the S, Goss (“G” in the figure legends) and Cu components are 20%, 11% and 3%, respectively. The fraction of the cube texture in this material is negligible,  $< 0.1\%$ , while the fraction of the other (random) orientations is significant, 15%.

#### 3.2 Evolution during annealing

Figure 2 and Figure 3 demonstrate that the microstructure is partially recrystallized ( $f_{\text{Rec}}=16\%$ ) already after 10 min of annealing at  $200^\circ\text{C}$ . At this early stage of recrystallization, nucleation takes place predominantly within bands consisting of lamellae with a large variety of orientations (many of



which are random orientations) and within shear bands, which are preferential nucleation sites for Goss- and Q-oriented grains. The fraction of the Bs component decreases significantly during annealing, while the fraction of random orientations increases (see Fig.4). Considerable changes are also observed within non-recrystallized regions: the lamellar structure coarsens from ~250 nm to 630 nm along the normal direction within the first 10 min of annealing (cf. Fig.1 and Fig.2). In addition, in this annealed sample the number density of particles is obviously higher than that in the as-rolled condition (cf. Fig.1a and Fig.2a), indicating the process of precipitation during annealing. Whereas most of these precipitates are observed along the lamellar boundaries (Fig.2a), in some cases, precipitates are also seen within recrystallized grains, decorating boundaries of lamellae consumed during recrystallization.

The process of precipitation can additionally be evaluated via changes in the electrical conductivity. Figure 5 shows that after the first 10 min of annealing the electrical conductivity increases from 31.2 to 33.1 MS/m, which is consistent with the observed increase in the particle number density. Although a certain reduction in the dislocation density taking place during annealing could also contribute to the increased conductivity, this contribution in aluminum is rather small [22] compared to that caused the precipitation process.

The size and area fraction of recrystallized grains increase with increasing annealing duration (see Figs.6-8). After 40 min of annealing the fraction of the recrystallized microstructure is significant,  $f_{\text{Rex}}=40\%$ . Nevertheless, the pattern of recrystallized grains growing preferentially within shear bands and within horizontal bands consisting of different crystallographic orientations is still clearly observed in this sample (Fig.7a). Compared to the sample annealed for 10 min, annealing for 40 min results in increased fractions of the Goss, Q and random orientations (see Fig.4). The electrical conductivity

continues to increase rapidly, reaching 35 MS/m after 40 min of annealing, followed by a slower increase beyond 40 min of annealing (see Fig.5).

After 2 h of annealing,  $f_{\text{Rex}}$  is 70%, and it is no longer possible to clearly identify where shear bands were located before annealing (Fig.7b). At this stage, the fraction of the Goss-component is already above 30%, and many recrystallized grains belonging to the Goss texture become neighbors with other Goss-oriented grains, thus forming LABs between them.

The area fraction of the Goss texture increases during further annealing between 8 h and 48 h at 200 °C (see Fig.4 and Fig.8). After 48 h of annealing, the material is fully recrystallized with an average grain size of 28  $\mu\text{m}$  (Fig.8b). The area fraction of the Goss texture in the fully recrystallized condition is 44%.

## Discussion

### 4.1 Strong Bs component in the rolling texture

The dominance of the Bs component in the deformation texture of the rolled material can be both due to a very large initial grain size retained after hot-forging and due to the presence of increased concentrations of the near-Goss orientation before rolling (see Section 2). A coarse-grained material is prone to shear banding [23], which can further enhance the Goss texture [24]. During continued rolling the Goss component rotates towards the Bs component [24], thus increasing the intensity of the latter. A typical result of such an evolution is a rolling texture where a strong Bs component is combined with a weaker Goss orientation and other rolling texture components. This combination is also observed in the present material, where the Bs and Goss orientations occupy 51% and 11% of the area, respectively. In the following, we shall consider how a strong Goss texture develops in this material during annealing.

#### 4.2 Nucleation of Goss and other grains in the beginning of recrystallization

In order to analyze why Goss-oriented crystallites nucleate preferentially in the beginning of recrystallization, we calculated the stored energy  $E_s$  from the EBSD data [16,17] collected after rolling in areas with different orientations. For Goss- and randomly oriented areas,  $E_s$  was much lower,  $0.29 \text{ MJ/m}^3$  and  $0.35 \text{ MJ/m}^3$ , respectively, than for the dominant Bs component,  $E_s = 0.7 \text{ MJ/m}^3$ . This result is consistent with previous X-ray experiment data for rolled copper, where Goss-oriented regions were found to contain a much lower dislocation density than regions of the Bs component [25]. Thus, there is a driving force for lower-energy Goss-oriented regions and regions of random orientations to grow into neighboring Bs-oriented matrix with a higher stored energy.

In the samples annealed for 10 min and 40 min, Goss- and Q-oriented grains predominantly nucleate at shear bands (Fig.2b, Fig.3 and Fig.7a). This observation supports earlier suggestions of Engler and co-workers [4,11,12] as well as experimental findings of Duckham et al. [13]. It is significant that whereas only a few Goss- and Q-oriented grains were identified at shear bands using a semi-automated EBSD technique in Ref.[13], our fully automated measurements covering large sample areas provide clear evidence that in the present material shear bands are the primary source of the Goss- and Q-oriented grains in the beginning of recrystallization.

Analysis of boundaries between recrystallized grains and their recovered environment (Rex/Rec boundaries) conducted for the 10 min-sample reveals that for the Goss-oriented grains the highest frequency of misorientation angles associated with such boundaries are within  $25\text{--}35^\circ$  with a dominance of the  $\langle 110 \rangle$  misorientation axes (Fig.9a). These misorientations are close to the ideal Goss/Bs  $35^\circ \langle 110 \rangle$  misorientation. Grains of the Q orientation have a high frequency of Rex/Rec boundaries in the range  $45\text{--}50^\circ$  with a broad distribution of misorientation axes (Fig.9b). The

distribution of misorientation axes for the Rex/Rec boundaries in the “random orientations” group (Fig.9c) is similarly broad to that in Fig.9b. Also, the distribution of misorientation angles in Fig.9c is similar to that for the Q-oriented grains, although the peak near  $45^\circ$  is not as sharp as in Fig.9b. In contrast, Rex/Rec boundaries of grains in the Bs+S+Cu group are characterized by a higher frequency of LABs (31%, see Fig.9d). Hence these grains are more likely to experience orientation pinning [26] during recrystallization, which can reduce their growth rate. Indeed, of all the analyzed texture components, the Bs+S+Cu group consistently has the smallest average recrystallized grain size after each annealing treatment (see Fig.10).

#### 4.3 Influence of precipitates

The particles observed in the microstructure of the as-rolled material most likely precipitated both at grain boundaries during heating of the ingot prior to forging and at some dislocation boundaries in the hot-forged microstructure before cooling. Therefore, it is suggested that the particles in the as-rolled microstructure are located at preexisting boundaries. In contrast, deformation-induced lamellae of different orientations and shear bands are almost free of particles. Upon annealing these regions recrystallize so quickly that the process of nucleation here is not affected by the precipitation, which provides grains nucleating in these regions an additional advantage during continued recrystallization. Whereas a large number of lamellar HABs can be pinned due to the additional precipitation taking place during annealing, sufficiently large recrystallized grains nucleated in the particle-free regions can sweep through particle-rich boundaries (see Fig.2).

#### 4.4 Changes between 40 min and 48 h of annealing

After 40 min of annealing the majority of shear bands and lamellar bands with a high frequency of random orientations are already recrystallized (see Fig.7a). During further annealing at 200 °C, the existing recrystallized grains grow into adjacent non-recrystallized regions. However, new nuclei can still appear in the remaining lamellar structures. In particular, in regions where Bs bands are interspersed with Goss-oriented subgrains, the latter can grow into the Bs matrix, as was also reported by Hjelen et al. [27]. An example of Goss-oriented nuclei in the Bs matrix after 40 min of annealing is presented in Fig.11. Such Goss/Bs-matrix nucleation, along with the growth of the recrystallized Goss grains formed earlier at the shear bands, leads to a rapid increase in the fraction of the Goss texture between 40 min and 2 h (see Fig.6). Due to continued nucleation of small Goss-oriented grains, the average grain size for this group remains slightly smaller than that of grains with random orientations up to 8 h of annealing (see Fig.10).

Between 8 h and 24 h Goss-oriented grains grow more rapidly than grains of any other orientation (see Fig.10). Note that after 8 h of annealing the material is almost fully recrystallized ( $f_{\text{Rex}}=91\%$ ). Therefore, very few new grains can nucleate, and the microstructure evolves largely by grain growth. At this stage, recrystallized Goss-oriented grains grow into grains of other orientations and form new low-energy LABs with other grains of the Goss component. As a result, the fraction of LABs increases from 19% in the recrystallized regions after 8 h to 26% after 48 h. This process resembles the process of grain growth in strongly cube-textured materials [28–30], though the fraction of LABs in our sample is significantly smaller than LAB fractions in such materials. Whereas the fraction of the Goss texture observed in the present study is greater than the corresponding fractions typically reported for Al-alloys, it is suggested that the strength of the Goss texture in these alloys can

further be increased by tuning the thermomechanical processing, which can have significant implications for their improved fatigue performance [31,32].

#### 4. Conclusions

The evolution of the microstructure and texture has been studied in the center layer of coarse-grained Al–0.3%Cu annealed at 200 °C after 95% cold rolling. The following conclusions are obtained in this study.

1. The deformed microstructure consists of a lamellar structure with an interlamellar spacing of approximately 250 nm, as measured using EBSD. Some of the lamellar boundaries are decorated by Al<sub>2</sub>Cu particles, which are considered to precipitate during thermomechanical treatments prior to cold rolling. The lamellar structures are intersected by shear bands.
2. Nucleation at shear bands is the primary source of the Goss- and Q-oriented grains in the beginning of recrystallization. Other preferential nucleation sites in the beginning of recrystallization are bands comprising lamellae with a large variety of crystallographic orientations. Nucleation in these locations seems unaffected by precipitation also taking place during annealing.
3. The fraction of the Goss-texture increases rapidly between 40 min and 2 h of annealing. This is attributed both to growth of the Goss-oriented grains nucleated earlier and to nucleation of new Goss grains in regions, where bands of the dominant Bs component are interspersed with Goss-oriented subgrains.
4. The average grain size of the Goss-oriented grains remains similar to those of the Q and random orientations up to 8 h of annealing. However, after annealing beyond 8 h Goss-oriented grains grow more rapidly than other grains. Between 8 h and 48 h of annealing the microstructure

evolves largely by grain growth. During this process Goss-oriented grains tend to consume grains of other orientations. This leads to the strengthening of the Goss texture, which in turn results in new low angle boundaries formed between recrystallized grains of the Goss component. After annealing for 48 h at 200 °C the area fraction of the Goss texture is 44%.

**Acknowledgements:** GLW and XH would like to acknowledge the National Natural Science Foundation of China (Nos. 51471039, 51327805 and 51421001). OVM thanks the support of the “111” Project (B16007) by the Ministry of Education and the State Administration of Foreign Experts Affairs of China.

## References

- [1] K. Ito, R. Musick, K. Lücke, *Acta Metall.* 31 (1983) 2137–2149.
- [2] J. Hirsch, K. Lücke, *Acta Metall.* 33 (1985) 1927–1938.
- [3] R.D. Doherty, L.-C. Chen, I. Samajdar, *Mater. Sci. Eng. A257* (1998) 18–36.
- [4] K. Lücke, O. Engler, *Mater. Sci. Technol.* 6 (1990) 1113–1130.
- [5] O. Daaland, E. Nes, *Acta Mater.* 44 (1996) 1413–1435.
- [6] O. Engler, P. Yang, X.W. Kong, *Acta Mater.* 44 (1996) 3349–3369.
- [7] O.V. Mishin, D. Juul Jensen, N. Hansen. *Metall. Mater. Trans. A* 41 (2010) 2936–2948.
- [8] K. Huang, K. Marthinsen, *Mater. Charact.* 110 (2015) 215–221.
- [9] K. Huang, K. Zhang, K. Marthinsen, R.E. Logé, *Acta Mater.* 141 (2017) 360–373.
- [10] H. Jazaeri, F.J. Humphreys, *Acta Mater.* 52 (2004) 3251–3262.
- [11] O. Engler, *Textures and Microstr.* 23 (1995) 61–86.
- [12] O. Engler, J. Hirsch, K. Lücke, *Acta Metal. Mater.* 43 (1995) 121–138.

- [13] A. Duckham, O. Engler, R.D. Knutsen, *Acta Mater.* 50 (2002) 2881–2893.
- [14] Q. Zhao, Z. Liu, S. Li, T. Huang, P. Xia, L. Lu, *J. Alloys Compd.* 691 (2017) 786–799.
- [15] X.R. Li, A. Wakeel, T.L. Huang, G.L. Wu, X. Huang, *IOP Conf. Series: Mater. Sci. & Eng.* 89 (2015) 012032.
- [16] A. Godfrey, W.Q. Cao, N. Hansen, Q. Liu, *Metall. Mater. Trans. A* 36 (2005) 2371–2378.
- [17] A. Godfrey, N. Hansen, D. Juul Jensen, *Metall. Mater. Trans. A* 38 (2007) 2329–2339.
- [18] W.T. Read, *W. Shockley: Phys. Rev.* 78 (1950) 275–289.
- [19] W.T. Read, *Dislocation in Solids*, McGraw-Hill, New York (1953) 155–172.
- [20] F.J. Humphreys and M. Hatherly: *Recrystallization and Related Annealing Phenomena*, Elsevier, Oxford, 2004.
- [21] G.L. Wu, D. Juul Jensen, *Mater. Charact.* 59 (2008) 794–800.
- [22] D. Trattner, M. Zehetbauer, V. Gröger, *Phys. Rev B* 31 (1985) 1172–1173.
- [23] A.A. Ridha, W.B. Hutchinson, *Acta Metall.* 30 (1982) 1929–1939.
- [24] O. Engler, J. Hirsch, K. Lücke, *Acta Metall.* 10 (1989) 2743–2753.
- [25] P. Gerber, J. Tarasiuk, T. Chauveau, B. Bacroix, *Acta Mater.* 51 (2003) 6359–6371.
- [26] D. Juul Jensen, *Acta Metall. Mater.* 43 (1995) 4117–4129.
- [27] J. Hjelen, R. Ørsund, E. Nes, *Acta Metall Mater.* 39 (1991) 1377–1404
- [28] O.V. Mishin, G. Gottstein, *Mater. Sci. Eng. A* 249 (1998) 71–78.
- [29] A.C. Wulff, O.V. Mishin, J.-C. Grivel, *J. Alloys Compd.* 539 (2012) 161–167.
- [30] H. Tian, H.L. Suo, A.C. Wulff, J.-C. Grivel, O.V. Mishin, D. Juul Jensen, *J. Alloys Compd.* 601 (2014) 9–13.
- [31] Z. Liu, F. Li, P. Xia, S. Bai, Y. Gu, D. Yu, S. Zeng, *Mater. Sci. Eng. A* 625 (2015) 271–277.



- [32] F. Li, Z. Liu, W. Wu, P. Xia, P. Ying, Q. Zhao, J. Li, S. Bai, C. Ye, Mater. Sci. Eng. A 669 (2016) 367–378.

ACCEPTED MANUSCRIPT

**Figure captions:**

**Figure 1.** Microstructure of 95% rolled Al–0.3%Cu: (a) BSE image showing lamellar structures and a shear band (marked by a dashed line). (b) a high magnification BSE image showing particles (bright features); (c) orientation map obtained using EBSD, where random orientations are shown in gray and where LABs and HABs are shown as white and black lines, respectively. The RD is parallel to the scale bar.

**Figure 2.** Microstructure of the Al–0.3%Cu alloy annealed at 200 °C for 10 min: (a) BSE image, where precipitates are seen as bright features; (b) orientation map showing coarsened lamellar structures and several recrystallized grains. Note a coarse Goss-oriented grain, which nucleated at a shear band and grew to a large extent along the RD (parallel to the scale bar). Orientations that do not belong to any orientation listed in the color code are represented by different shadings of gray. LABs and HABs shown as white and black lines, respectively.

**Figure 3.** Orientation map from a large region in Al–0.3%Cu annealed at 200 °C for 10 min. The map demonstrates a spatially non-uniform distribution of recrystallized grains which nucleate preferentially at shear bands and within horizontal bands containing a large frequency of random orientations shown by different shadings of gray. LABs and HABs are shown as white and black lines, respectively. The RD is parallel to the scale bar.

**Figure 4.** Fractions of different crystallographic orientations calculated from the EBSD data for Al–0.3%Cu annealed for different periods of time at 200 °C.

**Figure 5.** Electrical conductivity of Al–0.3%Cu as a function of annealing time at 200 °C.

**Figure 6.** Evolution of the area fraction of recrystallized grains in Al–0.3% Cu annealed at 200 °C.

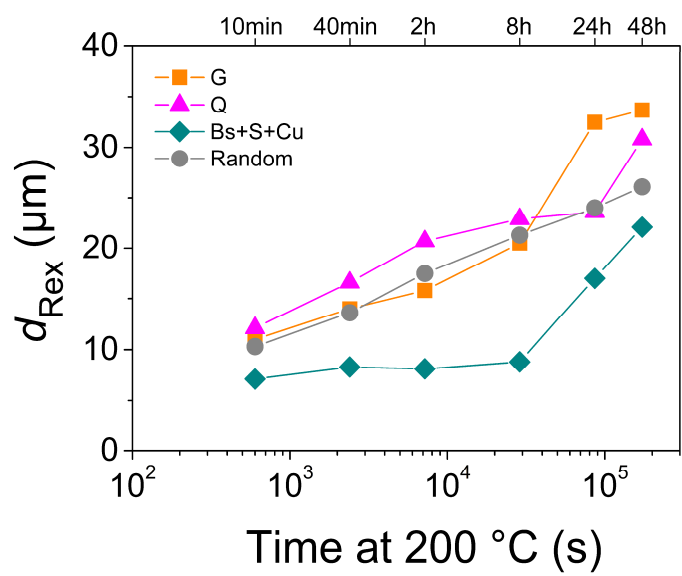
**Figure 7.** Orientation maps showing the microstructure in Al–0.3%Cu annealed at 200 °C for 40 min (a) and 2 h (b). Orientations that do not belong to any orientation listed in the color code are represented by different shadings of gray. LABs and HABs are shown as white and black lines, respectively. The RD is parallel to the scale bar.

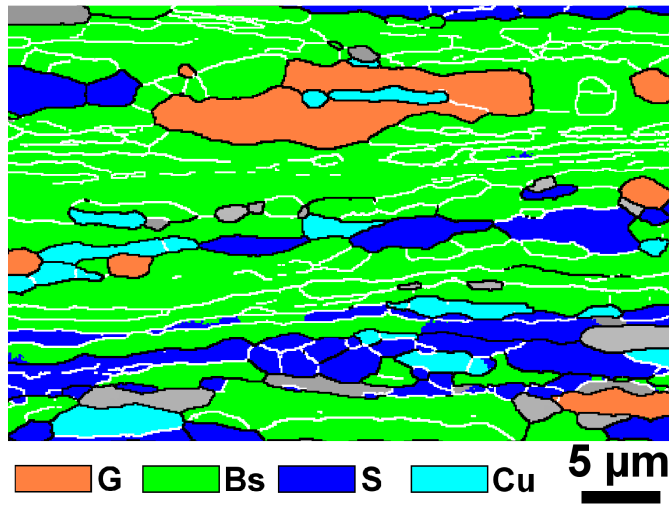
**Figure 8.** Orientation maps showing the microstructure in Al–0.3%Cu annealed at 200 °C for 8 h (a) and 48 h (b). Orientations that do not belong to any orientation listed in the color code are represented by different shadings of gray. LABs and HABs are shown as white and black lines, respectively. The RD is parallel to the scale bar.

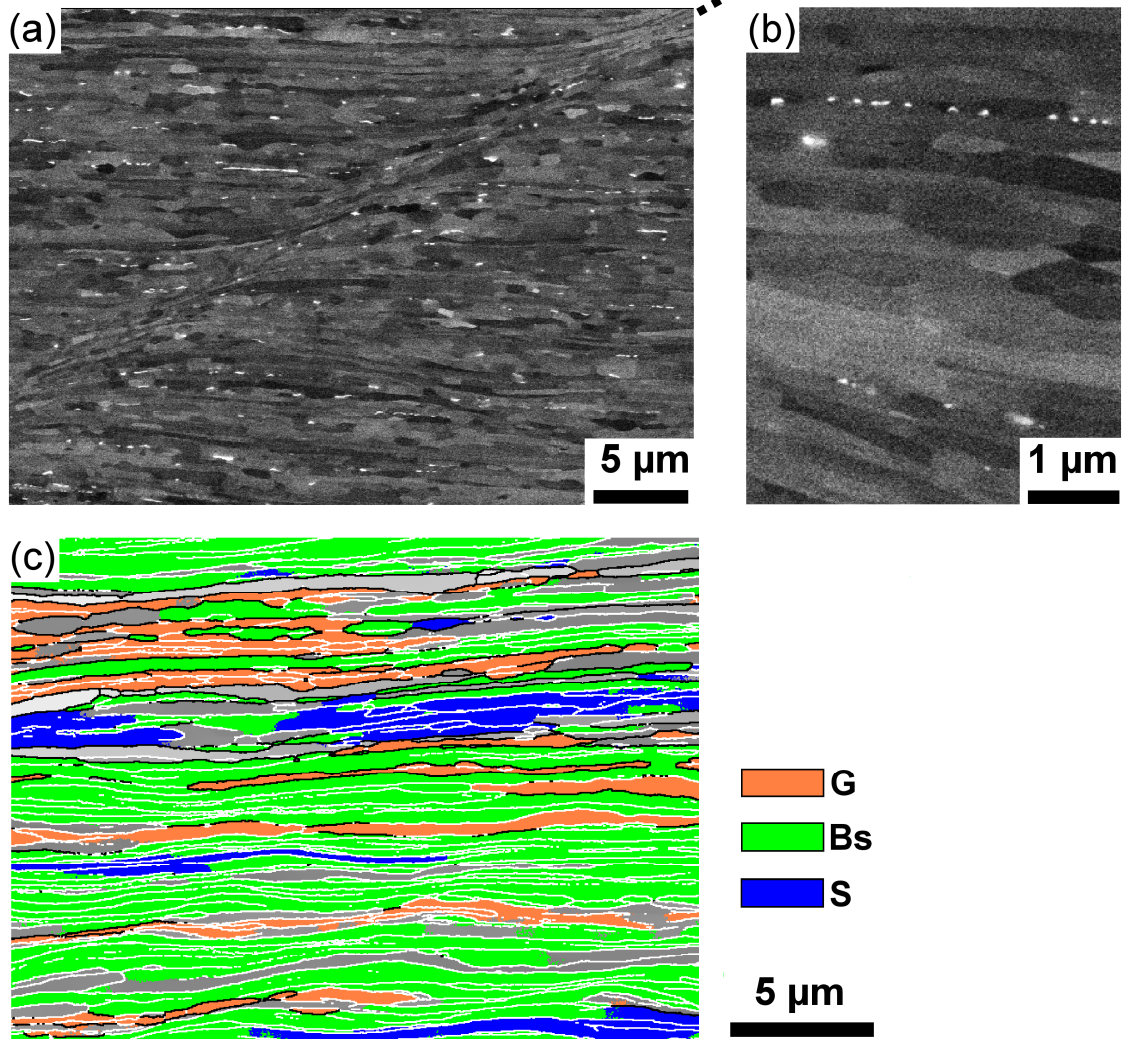
**Figure 9.** Distributions of misorientations across boundaries between recrystallized grains of different orientations and their recovered environment in the sample annealed for 10 min at 200 °C: (a) Goss-oriented grains; (b) Q-oriented grains; (c) grains of random orientations; (d) grains of the Bs, S and Cu components. Contour levels: 1, 2.

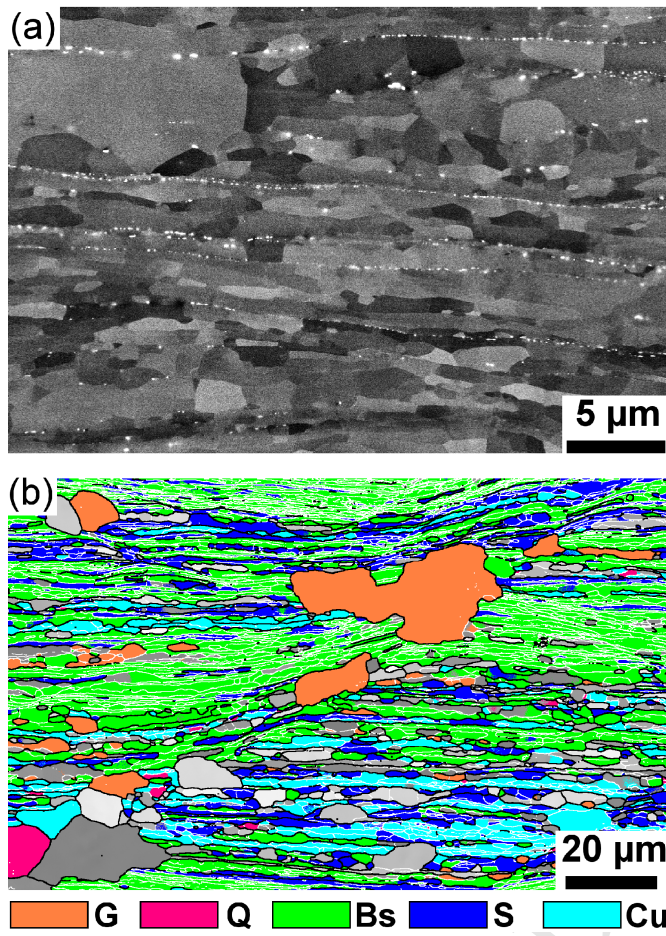
**Figure 10.** Evolution of the average size of recrystallized grains of different orientations in Al–0.3%Cu annealed at 200 °C.

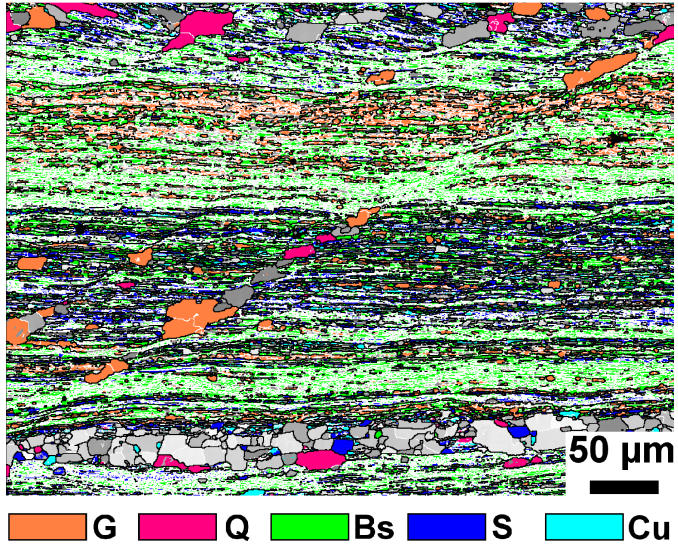
**Figure 11.** Goss-oriented crystallites in the Bs-dominated matrix after 40 min of annealing at 200 °C. LABs and HABs are shown as white and black lines, respectively.



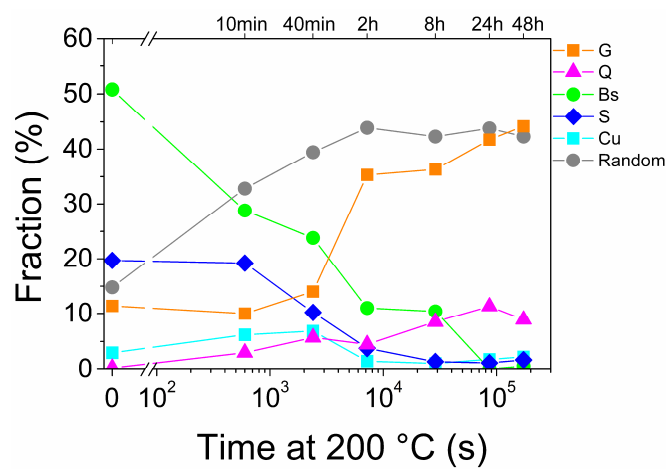


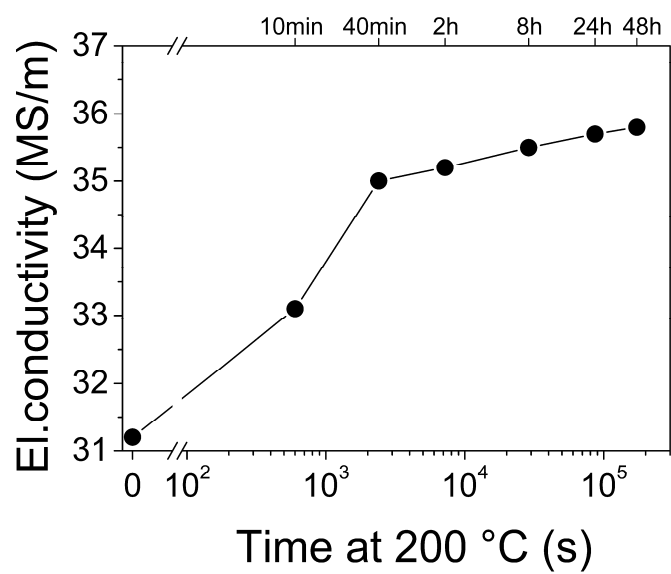


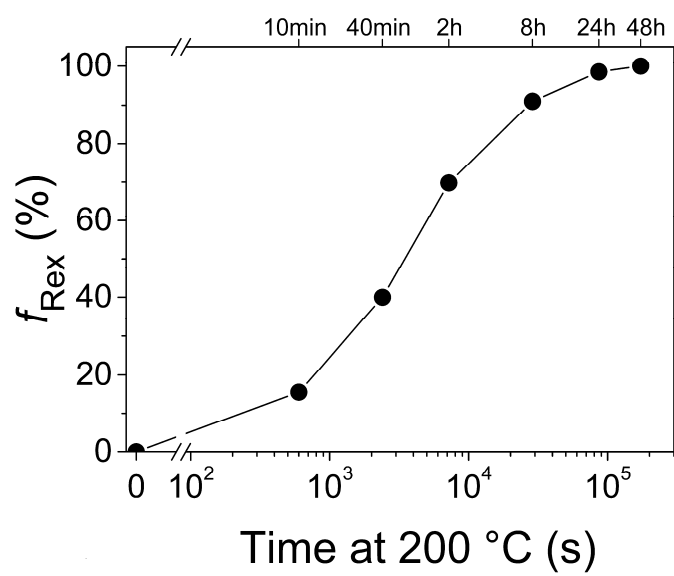


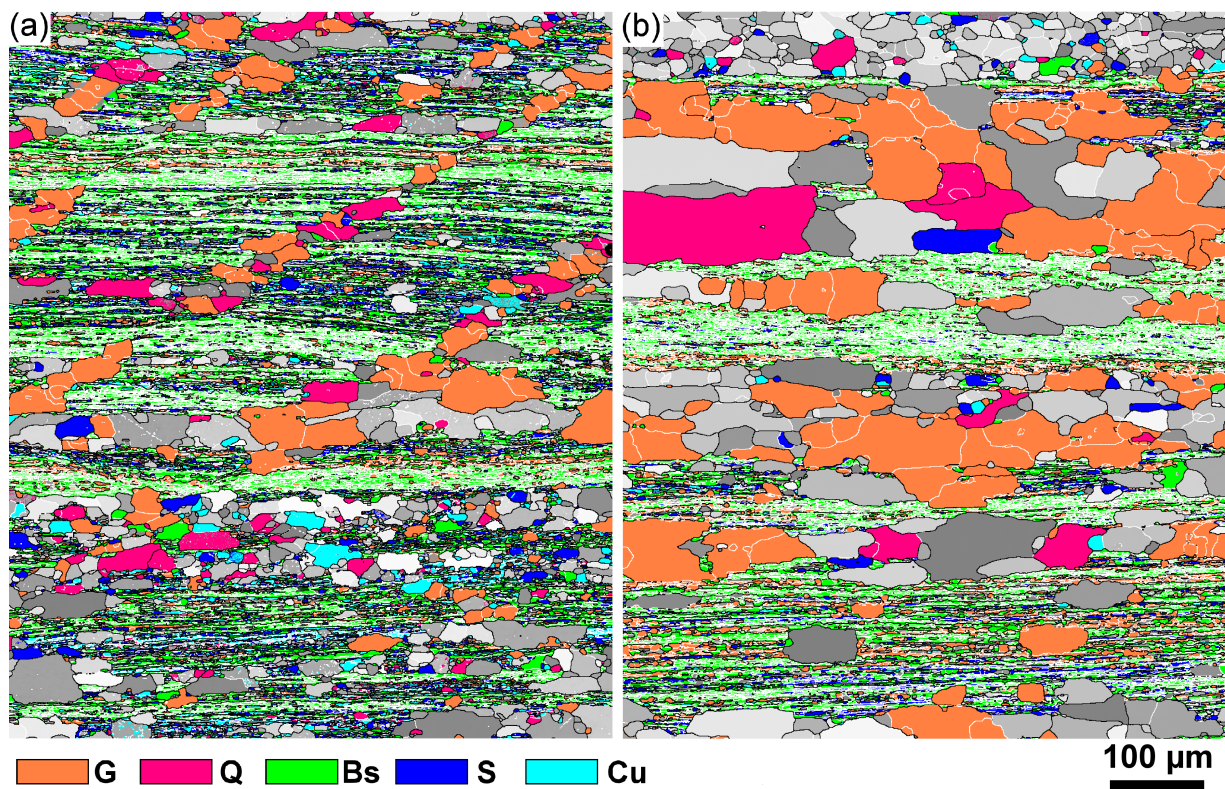


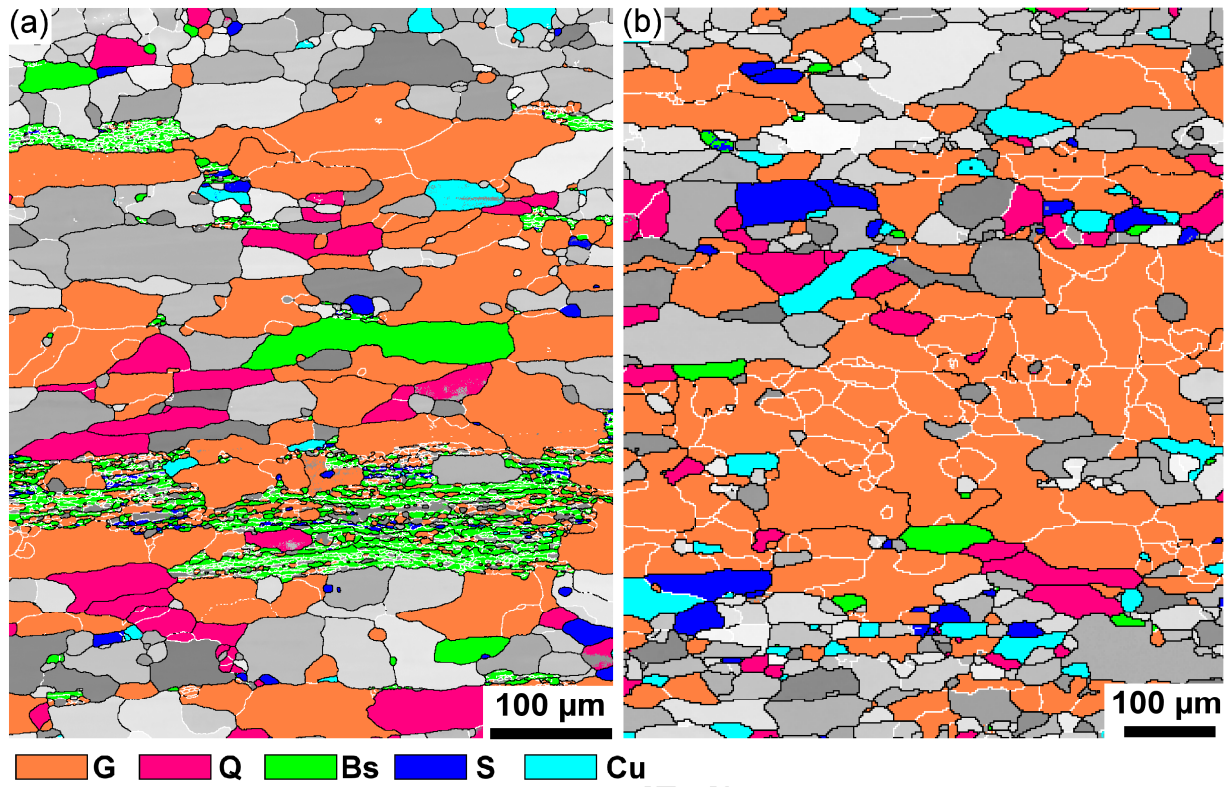


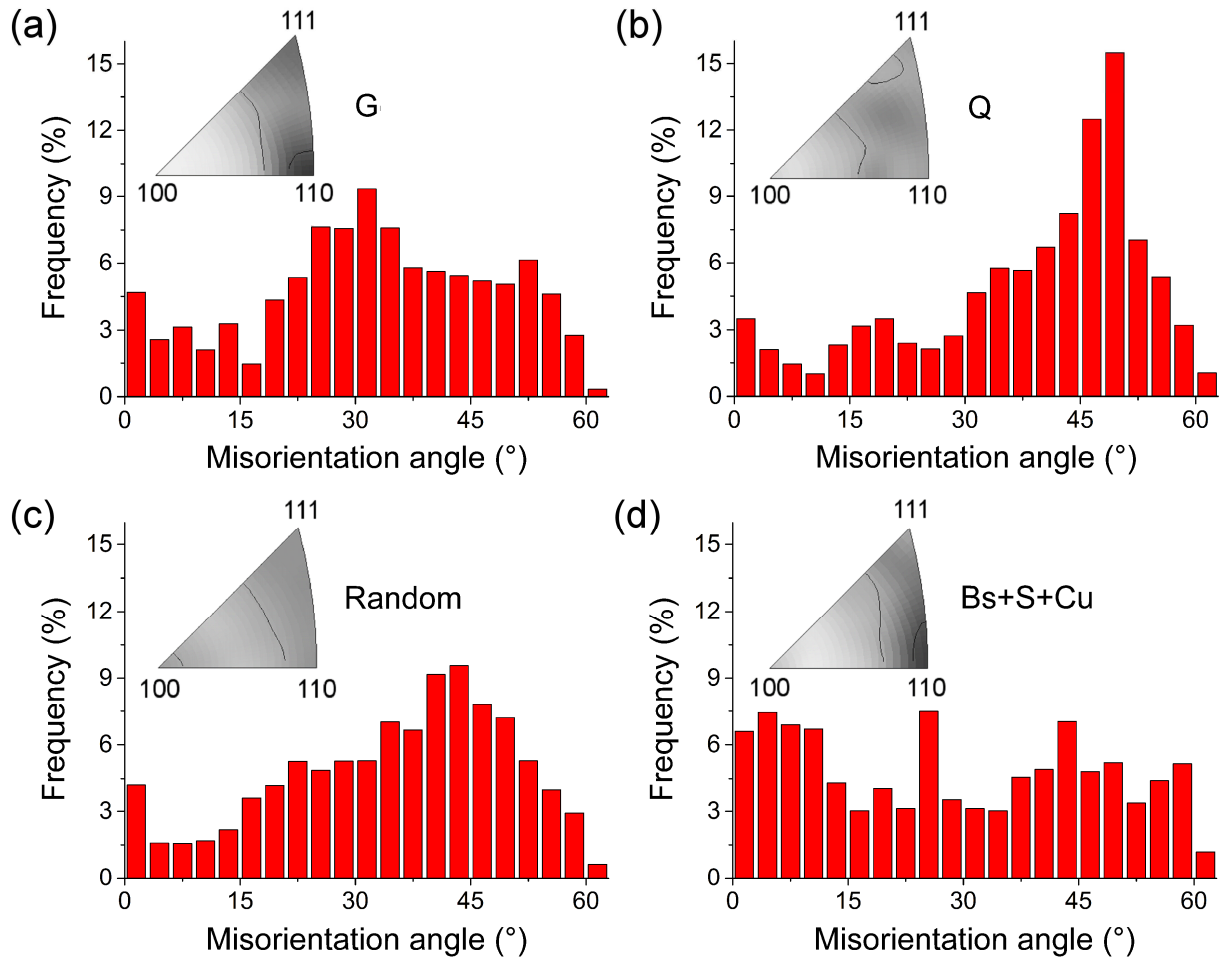












**Highlights:**

- Recrystallization in 95% rolled Al-0.3%Cu occurs during annealing at 200 °C
- Nucleation of Goss- and Q-oriented grains takes place primarily at shear bands
- The area fraction of the Goss texture in the fully recrystallized condition is 44%
- Strengthening of the Goss texture leads to an increased fraction of LABs